VARIATIONS WITHIN THE NORTHERN IMBRIUM NORITIC DEPOSITS. P. J. Isaacson and C. M. Pieters, Dept. of Geological Sciences, Brown University, Providence RI 02912. [Peter_Isaacson@brown.edu].

Introduction: The Imbrium basin is one of the most important and prominent geological features on the Moon. Filled with mare basalt, it is one of the largest and youngest basins, and its formation has influenced much of the geology of the lunar nearside. Thus, any interpretation of nearside geology must take into consideration the dominance of Imbrium and its associated ejecta deposits [1,2,3,4,5,6].

This study explores a group of deposits found north of Mare Frigoris (region shown in Figure 1). Previous analysis of this region using Clementine 5-band reflectance spectra found these deposits to be anomalous relative to their surroundings due to their noritic composition [7]. Similar lithologies have been found surrounding other lunar basins [8], but our analysis shows the deposits analyzed here to be distinct from others around Imbrium [2, 3]. Four large post-Imbrium craters have formed in this northern region (central peaks shown in Figure 1). As craters excavate to different depths based on their size [9], these large craters provide a window to different depths of the local crust, and thus provide constraints on the stratigraphic relationships of the deposits. Smaller craters are used to analyze the deposits in other contexts such as near-surface composition. The goal of this study is to better characterize the composition, regional extent and heterogeneity, and stratigraphy of the North Imbrium Noritic (NIN) deposits.

Methods/Data: Clementine UVVIS multispectral reflectance data was the primary data source for this study. Careful analysis was performed on craters of various size ranges, in both the mare and the highlands. The region is characterized by three principal rock types: anorthosite, mare basalt, and anorthositic norite. Figure 2 presents characteristic 5-band spectra for each principal material found in the region. Crater maturity (based on morphology and spectral properties [10]) was examined to ensure comparison of similar materials. Representative spectra of the large crater central peaks were analyzed to determine trends with depth and selenographic position. Regional trends in surface

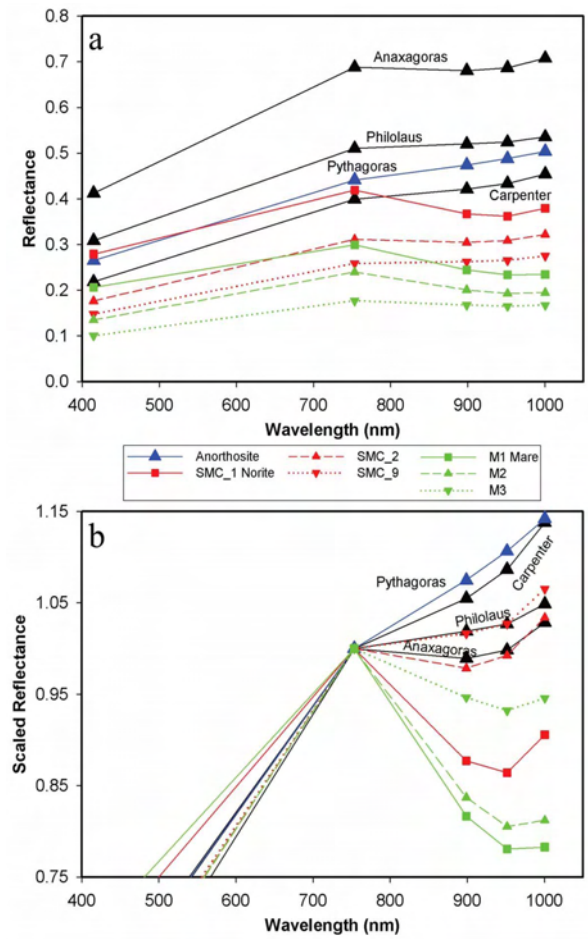

Fig. 2: Clementine 5-band spectra for central peaks (labeled) and principal rock types (colors). (**a**) Reflectance. Maturity trends in norite (red) and mare (green) are indicated by solid (fresh), dashed (intermediate), and dotted (degraded) lines. (**b**) Scaled reflectance (same spectra as **a**). Spectra have been scaled (multiplicative) to unity at 750 nm. This scheme emphasizes trends in band strength and shape, which are apparent for all three suites of spectra. Band strength decreases with maturity in norite and mare, and generally with crater size (Figure 1) in central peaks.

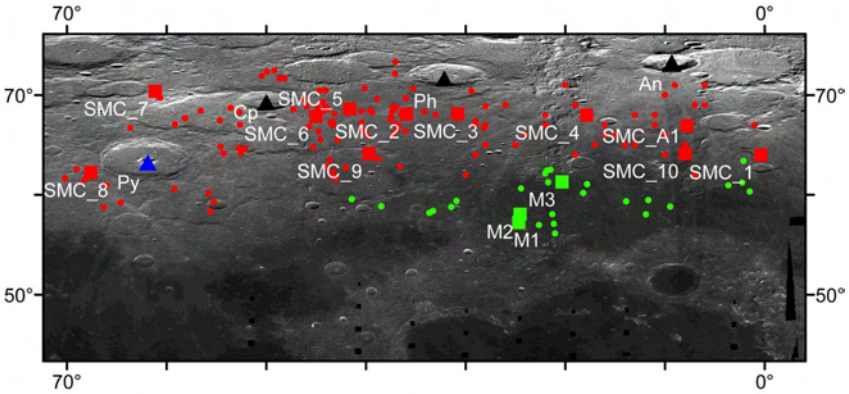

Fig. 1: NIN region. Base image is a Clementine 750 nm albedo image in a simple cylindrical projection. The northern portion of Imbrium basin is visible at the bottom of the image. Suites of small crater spectra analyzed are indicated by dots (green for mare, red for anorthositic norite (NIN)). Larger symbols indicate example spectra used in Figs. 2 & 3. Labels for these special craters are in white. The four large craters are indicated by triangles (central peak spectra). Their diameters in km are (west to east): 130 (Pythagoras), 59 (Carpenter), 70 (Philolaus), 50 (Anaxagoras).

geology were determined with a suite of 5-band spectra from more than 140 small craters (1-10 km). Locations and sizes of craters used in the study are shown in Figure 1.

Results: The spectroscopic difference between mare basalt and anorthositic norite is clear; noritic materials are characterized by an upturn in the 1000 nm band, due to the greater abundance of low-Ca pyroxene, which causes a shorter wavelength absorption [11, 12]. Mare basalts have a longer wavelength absorption due to more abundant high-Ca pyroxene. Central peaks appear to become more feldspathic with depth as inferred from crater diameter [9], except for Carpenter and Philolaus, where this trend is reversed (Carpenter is smaller and therefore shallower, but appears to be more feldspathic). Lastly, the composition of Pythagoras' central peak is clearly distinct, as it alone is composed of almost pure anorthosite.

The small craters reveal a general trend in composition from more noritic in the east to more feldspathic in the west, based on the character and overall strength of the pyroxene absorption. Figure 3 presents some of the best and most representative spectra extracted from the entire suite (see Figure 1). Maturity effects (see Figure 3) are separated through analysis of a large group of similar craters. Compositional heterogeneity is observed, and the trend is not perfect (some eastern craters have weaker bands than western craters). However, the overall trend is of decreasing norite/plagioclase from east to west.

Discussion: These results imply a regional two-layered stratigraphic model, with a noritic layer (best exposed by small craters) overlying more feldspathic materials. The maximum thickness of the noritic layer is constrained by the central peak origin depth of Pythagoras, as its central peak is the only point where the underlying feldspathic material is fully exposed. Superimposed on this regional trend are additional complexities that can be summarized best with two competing hypotheses.

Regional depositional heterogeneity. The observed east-west trend in surface composition appears to indicate that the NIN deposits are characterized by a regional (longitudinal) gradation in composition. Previous work has suggested that Imbrium deposits may be extremely heterogeneous [1,2,3], a conclusion supported by the current results. Regional heterogeneity could also be coupled to depositional history involving both early South Pole-Aitken Basin (SPA) antipodal [13] and later Imbrium deposits.

Vertical heterogeneity. The central peak data generally support variations in the thickness of the noritic zone (but not as a continuous trend). Heterogeneity has been observed on the scale of individual central peaks [14], so heterogeneity on the scale of different crater depths is certainly possible.

Although the data are not fully described by either one of these hypotheses for the stratigraphy and regional extent of the NIN deposits, a hybridization of the two could result in a self-consistent explanation. This excludes a simple model for regional stratigraphy, as deposits appear to grade in composition regionally as well as vertically. Vertical heterogeneity can be explained by heterogeneous mixing during depositional processes leading to incorporation of varying amounts of underlying feldspathic material. The composition of the surface material also varies regionally, which leads to different lithologies at similar depths across the region.

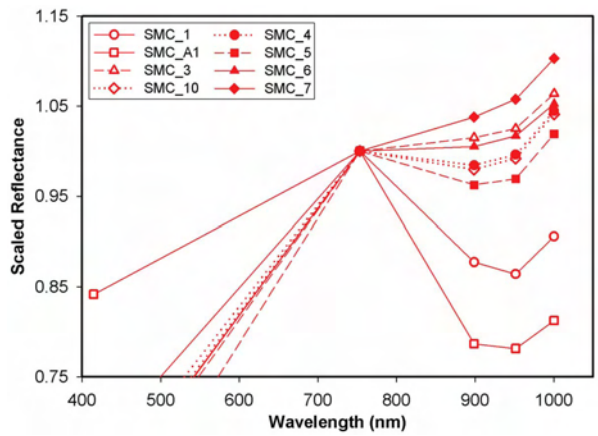

Fig. 3: Surface trends in spectra from small craters. Open points are farther east, closed west, and trend east-west down the legend columns. Most spectra are from craters of intermediate maturity, and maturity differences support the regional trend: 1 and A1 are fresh (explaining extreme band strengths), 10 is degraded and far east with a strong band while 4 is fresher and farther west with a weaker band, and 5 is fresher and very far west, probably why it is inconsistently strong. 3 is very degraded, which helps explain its weak band relative to others in the eastern region.

Summary and Conclusions: The NIN deposits were analyzed using Clementine 5-band reflectance spectra. A heterogeneous noritic surface appears to overly an anorthositic substrate. Compositional variations of materials within the region were identified both with depth and with selenographic longitude. The results suggest two processes (source heterogeneity, heterogeneous depositional mixing), both of which are important in the evolution of these deposits.

References: [1] Spudis, P.D. et al. (1988) *PLPSC XVIII*, 155-168. [2] Bussey, D.B.J. et al. (1998) *LPS XXIX*, 1352. [3] Spudis, P.D. et al. (1999) *LPS XXX*, 1348. [4] Haskin, L.A. (1998) *JGR, 103*, 1679-1689. [5] Lucchitta, B.K. (1978) *USGS Map* I-1062. [6] Wilhelms, D.E. (1987) *USGS Prof. Paper* 1348. [7] Pieters, C.M. (2002) *LPS XXXIII*, 1776. [8] Hawke, B.R. et al. (2003) *JGR, 108 (E6)*. [9] Melosh, H.J. (1989), *Oxford U. Press*, 245pp. [10] Lucey, P.G. et al., (2000), *JGR, 105*, 20377-20386. [11] Pieters, C.M. (1986), *Rev. Geophys.*, 24, 557-578. [12] Burns, R.G., (1993). *Remote Geochemical Analysis*, 3-29. [13] Petro, N.E. and Pieters, C. M. (2006) *these proceedings.* [14] Tompkins, S. and Pieters, C.M. (1999) *MAPS, 34*, 25-41.

Acknowledgements: The authors would like to acknowledge the support of NASA grant NNM05AB26C.